Beyond Terabit/s/λ Nonlinearity-free Transmission over the Hollow-core Fiber

Yang Hong, *Member, IEEE*, Sylvain Almonacil, *Member, IEEE*, Haik Mardoyan, *Senior Member, IEEE*, Carina Castineiras Carrero, Sergio Osuna, Javier R. Gomez, David R. Knight, *Member, IEEE*, and Jeremie Renaudier, *Senior Member, IEEE*

***Abstract*—In this paper, we demonstrate the beneficial ultra-low nonlinearity and ultimate-low latency of hollow-core fibers (HCFs) through transmission of 130-GBaud Terabit/s/λ wavelength-division multiplexed (WDM) signals in an optical recirculating loop. A comparative study has been performed by inserting either a ~1.1-km length of HCF or a matched length of single-mode fiber (SMF) as the fiber under test into the loop. The transmission performance of both dual-polarization 16-ary quadrature amplitude modulation (DP-16QAM) and DP probabilistic constellation shaping 64-ary QAM (DP-PCS-64QAM) are presented. We show that the HCF can accommodate nonlinearity-free transmission for the 130-GBaud Terabit/s/λ signals under a launch power up to 23 dBm (~13.5 dBm/channel). As such, after 25-loop transmission with a 23-dBm launch power, more than 2-dB signal-to-noise ratio improvement and ~17.4% higher capacity can be achieved. In the meantime, the >30% lower latency of the HCF is directly validated through the comparison of the power monitoring traces of the SMF-/HCF-based optical recirculating loop. Finally, we perform a field trial of 90.22-GBaud 16QAM transmission over a ~1.4-km length of deployed HCF cable, confirming the practical applicability of using the HCF for high-capacity low-latency optical transmission.**

***Index Terms*—Hollow-core Fibers; Ultrahigh-rate Coherent Transmission; Fiber Nonlinearities; Low-latency Optical Communications.**

I. Introduction

THE optical network infrastructure, empowered primarily by the solid-core single-mode fibers (SMFs), has been underpinning optical communications over the past decades [1-2]. However, there is a persistent demand for higher capacity and lower latency, both of which are particularly desirable for data-hungry and latency-sensitive applications, such as large-scale data center interconnections, ultrahigh-definition video streaming, and cloud/edge computing [2]. In light of this, enormous efforts have been made to boost the capacity of optical fiber communication systems, including the proposals of various optical/digital signal processing (DSP) techniques, massive parallel transmission through spatial-division multiplexing over multi-core and/or multi-mode fibers, as well as ultra-wideband transmission using novel optical amplifiers [3-6]. However, to date, it remains challenging to overcome/mitigate the intrinsic fiber nonlinearity of conventional solid-core fibers (such as SMFs and multi-core fibers), which ultimately restricts the achievable capacity. This is normally referred to as the nonlinear Shannon limit of optical fiber communication systems [7]. On the other hand, although it is known that the overall latency of optical links is dominated by the propagation time in transmission fibers [8], marginal improvements have been reported so far. For example, by using a small-core dual-cladding fiber design with a complex refractive index profile, only 0.3% latency reduction for SMFs has been reported [9]. This is due to that light speed in conventional solid-core fibers is fundamentally determined by the refractive index of the silica-glass core.

Recently, hollow-core fibers (HCFs) have attracted significant interests from both academia and industry and are arising as a promising solution for next-generation transmission fibers [10]. HCFs rely on a radically different light guidance mechanism and are capable of simultaneously addressing the nonlinearity and latency limitations of SMFs. Since light travels through a hollow core in HCFs rather than a solid glass core, HCFs constitute the ultimate low-latency transmission medium [11]. In the meantime, it has been demonstrated that HCFs can achieve a loss of 0.08±0.03 dB/km, representing the lowest loss record amongst any types of optical fibers to date [12]. Furthermore, the unique air-guided propagation property of HCFs also promises a much lower fiber nonlinearity than the solid-core SMF. In [13], the Kerr coefficient of a HCF was measured to be less than 2.2×10^{-23} m^2/W, which is around three orders of magnitude lower than that of the SMF (typically around 3×10^{-20} m^2/W). This can be translated into a superior tolerance to high launch powers into the fiber, thereby offering

Manuscript received xx XX 2024; revised xx XX 2024; accepted xx XX 2024. Date of publication xx XX 2024; date of current version xx XX 2024. (Corresponding author: Yang Hong.)

Y. Hong, S. Almonacil, H. Mardoyan, C.C. Carrero, and J. Renaudier are with Nokia Bell Labs, Massy, France (e-mails: yanghong@ieee.org; sylvain.almonacil@nokia-bell-labs.com; haik.mardoyan@nokia-bell-labs.com; carina.castineiras_carrero@nokia.com; jeremie.renaudier@nokia-bell-labs.com). Y. Hong is currently with Microsoft Azure Fiber, Romsey, United Kingdom.

S. Osuna is with the Network Infrastructure Division of Nokia, Madrid, Spain (e-mail: sergio.osuna@nokia.com).

J.R. Gomez is with Lyntia, Madrid, Spain (e-mail: jruizgo@lyntia.com).

D.R. Knight is with OFS Laboratories, Somerset, USA (e-mail: knightd@ofsoptics.com).

Color versions of one or more figures in this article are available at https://doi.org/XXXX.

Digital Object Identifier XXXX.

the potential to realize nonlinearity-free transmission. In other words, by adopting HCFs, it is possible to break the fundamental nonlinear Shannon limit experienced in SMFs.

In the literature, most of the HCF-based transmission experiments were based on a straight-line single-span link [13-21], and some of these adopted high launch powers to showcase the beneficial ultra-low nonlinearity of HCFs. For instance, it was demonstrated that for three-channel 400G signals, nonlinearity-penalty-free transmission could be achieved over ~10-km length of HCF under a launch power up to 20.3 dBm [14]. In comparison, in the case of the link with a matched length of SMF, only ~15 dBm could be tolerated without experiencing any nonlinearity-induced performance penalty. In [15], penalty-free transmission of 95-GBaud dual-polarization probabilistic constellation shaping 64-ary quadrature amplitude modulation (DP-PCS-64QAM) was demonstrated at 800 Gb/s/λ. The total launch power to the HCF was up to 28 dBm, which corresponded to around 12 dBm/channel. However, only a short HCF link of ~200 m was considered. A few works explored the use of the optical recirculating loop to investigate the transmission performance of HCFs [21-25], yet none of them studied the impact of fiber nonlinearity in the loop setup. In [22], a length of 4.76-km HCF was put inside the loop to investigate its performance improvement relative to the SMF and non-zero dispersion-shifted fiber for intensity-modulation and direct-detection systems. For coherent transmission, a few HCF-based recirculating loop experiments using 32-GBaud QPSK/16QAM signals have been conducted over the past few years [23-25]. The total launch power to the HCF was 20 dBm in a most recent demonstration [25], which corresponded to a launch power of ~3.9 dBm per channel for the 32-GBaud signals. In [21], 95-GBaud (800 Gb/s/λ) transmission was demonstrated over an HCF-cable-based loop, which to the best of our knowledge, represents the highest baud rate of coherent transmission reported to date.

In this paper, we report on the transmission of 130-GBaud Terabit/s/λ signals over an optical recirculating loop and expand upon the preliminary results presented in [26], through which we show the low nonlinearity and low latency of the HCF relative to SMF. Nonlinearity-free transmission of DP-16QAM and DP-PCS-64QAM signals over the HCF has been demonstrated under launch power levels up to 23 dBm (which equals to ~13.5 dBm/channel). It is shown that after 25-loop transmission with a 23-dBm launch power, >2-dB signal-to-noise ratio (SNR) improvement and ~17.4% higher capacity can be achieved, thanks to the ultra-low nonlinearity of the HCF. We further report on the use of use of monitoring pulses of the recirculating loop to directly assess the lower latency of HCF relative to SMF. This lower latency has also been validated through our field trial using a HCF cable, conforming that the HCF offers >30% latency reduction (~1.6 μs/km) relative to SMF. Fig. 1 compares recent HCF-based transmission experiments using either a single-span or recirculating loop setup. To the best of our knowledge, our work represents the first Terabit/s/λ transmission (and the highest baud rate ever reported) over the HCF. Note that in Fig. 1, the loop results of this work refer to the 130-GBaud PCS-64QAM transmission with a launch power of 23 dBm after 1 loop and 25 loops, respectively.

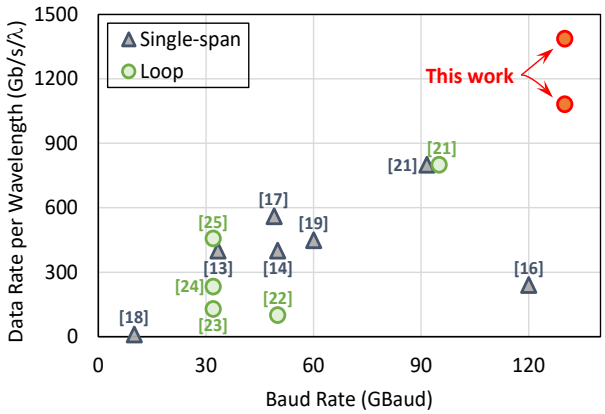

Fig. 1. Summary of some recent HCF-based transmission demonstrations.

The rest of this paper is structured as follows. Section II gives the details of the experimental setup and loss performance of the HCF used in this work. The performances of 130-GBaud DP-16QAM and DP-PCS-64QAM transmission are presented in Section III. Section IV compares the latency performance between the HCF and SMF, which also includes the results obtained through the field trial. Finally, Section V concludes this work.

II. Experimental Setup

The experimental setup of the optical recirculating loop is depicted in Fig. 2(a). The transmitter was composed of a channel under test (CUT) and eight wavelength-division multiplexing (WDM) comb channels emulated by a C-band amplified spontaneous emission (ASE) source. A tunable laser source (TLS) operated at 1559.39 nm was used as the optical

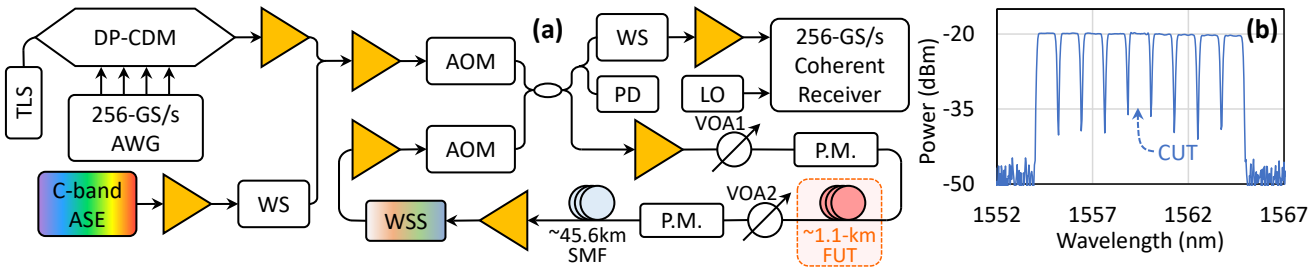

Fig. 2. (a) Experimental setup of the optical recirculating loop, and (b) optical spectra of the WDM channels at the transmitter.

carrier for a DP coherent driver modulator (DP-CDM). The TLS's linewidth is ~10 kHz. A 256-GS/s arbitrary waveform generator (AWG, 10-dB bandwidth is ~70 GHz) was used to modulate the DP-CDM to generate 130-GBaud signals for the CUT. The eight 130-GBaud neighboring comb channels were generated by using a WaveShaper (WS) to spectrally shape the amplified output of the C-band ASE source. The channel spacing of the WDM channels was 150 GHz. The amplified CUT and the comb channels were combined via an optical coupler, and then further amplified by an erbium-doped optical fiber amplifier (EDFA). Fig. 2(b) shows the optical spectra of the nine WDM channels at the transmitter. We note that the spectral range was chosen to match the low-loss transmission window of the used HCF in this work, which will be presented later in this section. The resulting optical signal was fed into the optical recirculating loop, which was controlled by two acousto-optic modulators (AOMs) by using two complementary control pulses.

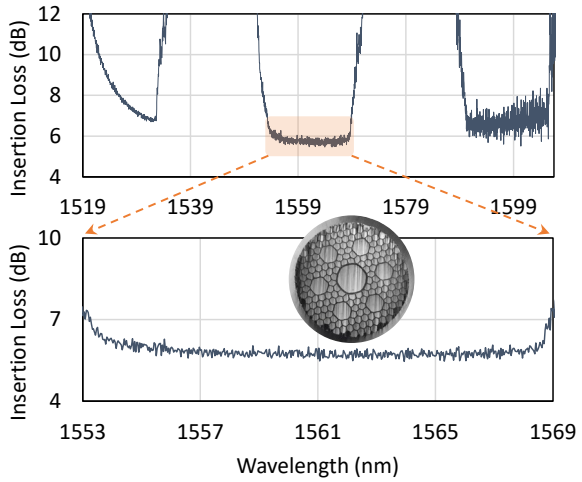

Fig. 3. Insertion loss performance of the ~1.1-km length of HCF (including the SMF-HCF interconnection losses). Inset: cross section view of the AccuCore HCF® microstructure core rod prior to fiber draw.

Inside the loop, a high-power EDFA together with a variable optical attenuator (VOA1) were used to vary the launch power into the fiber under test (FUT). An in-line power meter (P.M.) was placed in front of the FUT to monitor the level of the launch power. The FUT was either a spool of ~1.1-km SMF or a spool of ~1.1-km HCF. We adopted the standard SMF (ITU G.652) with a typical core geometry and its total insertion loss is around 0.2 dB at the wavelength of interest. As shown in the inset of Fig. 3, the HCF adopts the photonic bandgap design with six surrounding shunt cores to suppress the higher-order modes and multipath interference from modal crosstalk [18]. The core diameter of the HCF is typically ~25 µm and further details of the fiber can be found in [27]. Fig. 3 shows the insertion loss performance of the used HCF spool, which includes the loss of the ~1.1-km HCF itself and the HCF-SMF interconnection losses (~1 dB per fiber end) at both ends of the fiber spool. In the wavelength range of 1519 nm to 1606 nm, the HCF under study has three transmission windows that are separated by high loss regions at surface mode crossings where effective index matching and thus power transfer to highly lossy and dispersive surface modes occurs [28]. The middle window centered at ~1561 nm exhibits the lowest total loss of ~6 dB over a spectral width of around 15 nm (~1553.5 nm to ~1568.5 nm).

After the FUT, another VOA (VOA2) was used to adjust the optical power into the ~45.6-km buffering SMF. We note that this ~45.6-km SMF was used as the buffer to enable sufficient time for the execution of the recirculating loop. Another in-line P.M. was used in front of the buffering SMF to ensure that the optical power was fixed to 10.2 dBm in all cases, at which the buffering SMF's nonlinearity is expected to impose negligible impact on the transmission performance. Subsequently, a pair of EDFAs and a 50-GHz-grid wavelength-selective switch (WSS) were used to flatten the optical powers of the WDM channels, as well as balance the loss and gain of the loop. At the receiver side, 10% tap of the optical power from the output of the loop was fed into a photodetector (PD) for monitoring the power balance of the loop. The rest optical signal was filtered by another WS for CUT selection. The output of the WS was further amplified before been fed into a coherent receiver. Finally, a 256-GS/s real-time oscilloscope with a 3-dB bandwidth of ~110 GHz was used to capture the electrical outputs of the coherent receiver for offline DSP.

In this work, we considered both 16QAM and PCS-64QAM with an entropy of 5.7 bits/symbol as the modulation formats. In the transmitter DSP, the generated signal was Nyquist filtered by a root-raised-cosine filter with a roll-off factor of 0.01. To combat the bandwidth limitation of the transmitter, digital pre-emphasis was applied using the inverse of the CUT's optical spectrum after the DP-CDM. At the receiver side, the captured signal was processed by standard DSP [29], including matched filtering, chromatic dispersion compensation, polarization de-multiplexing using complex 2×2 adaptive equalization, carrier frequency offset compensation, carrier phase recovery, and least-mean square algorithm-based post-equalization. We note that no compensation for fiber nonlinearity was performed in the DSP. Finally, the de-modulated signals were used to calculate the bit error rate (BER), SNR, normalized generalized mutual information (NGMI), and achievable information rate (AIR).

III. Experimental Results

In this section, we present the experimental results of both 16QAM and PCS-64QAM transmission at 130 GBaud over the optical recirculating loop. To investigate the impact of the ~1.1-km FUT's nonlinearity on transmission, we have varied the level of launch power into the FUT and the number of recirculating loops. We note that when the ~1.1-km HCF is adopted as the FUT in the loop (together with the ~45.6-km length of buffering SMF), it is referred to as 'HCF loop', whereas 'SMF loop' corresponds to the case when a ~1.1-km SMF is used as the FUT. Specifically, BER and SNR are used as the metrics to evaluate the performance of the 16QAM transmission, whilst NGMI and AIR results of the PCS-64QAM transmission will be presented.

A. 130-GBaud 16QAM Transmission

Fig. 4 shows the BER and SNR performances versus launch power of the 16QAM transmission in the 'HCF loop'. It is seen in Fig. 4(a) that similar BER performance is achieved when varying the launch power from 19 dBm to 23 dBm at the same number of loops. Furthermore, this is achieved in all three scenarios, i.e., 1 loop, 10 loops, and 25 loops. Similarly, the SNR performance shown in Fig. 4(b) exhibits the same trend as that of the BER performance. As aforementioned, the optical power into the buffering SMF was always fixed to 10.2 dBm, regardless of the varying launch power into the FUT. In this regard, if the FUT's nonlinearity is sufficiently low, under the same number of loops, comparable transmission performance should be expected. Given that the results in Fig. 4 clearly indicate that no BER or SNR performance penalty is induced by the FUT (~1.1-km HCF in this case) even at a 23-dBm launch power after 25 loops, the nonlinearity of the HCF is confirmed to be negligible. It is worth noting that the maximum total launch power in this work (i.e., 23 dBm, which corresponds to ~13.5 dBm/channel) was limited by the available high-power EDFA when performing the experiments. We anticipate that the HCF should be able to support penalty-free transmission with even higher launch powers.

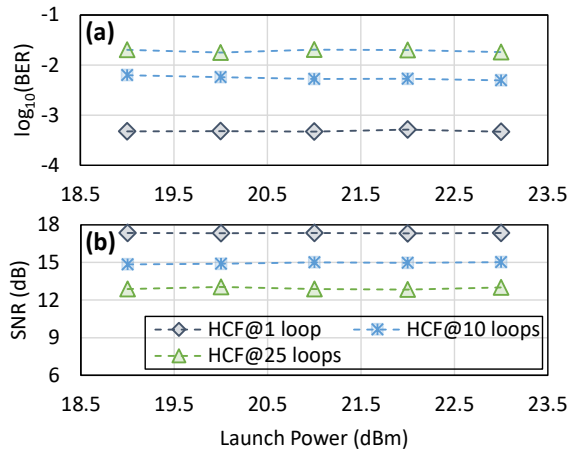

Fig. 4. Performance of 130-GBaud 16QAM transmission over the optical recirculating loop: (a) BER versus launch power, and (b) SNR versus launch power.

To reflect the ultra-low nonlinearity of HCF relative to SMF, we also adopted ~1.1-km length of SMF as the FUT in the loop and performed the 130-GBaud 16QAM transmission through the 'SMF loop'. The BER and SNR performance comparisons between the 'HCF loop' and 'SMF loop' are shown in Fig. 5(a) and Fig. 5(b), respectively. It is seen that after 1-loop transmission, when increasing the launch power from 13.5 dBm to 23 dBm, similar BERs and SNRs can be achieved by the 'SMF loop' as well. This implies that the FUT's nonlinearity (in this case, ~1.1-km SMF) is also negligible after 1 loop due to its very short length. However, when the number of loops is increased to 20, similar BERs and SNRs can only be maintained by keeping the launch power below 19 dBm. Obvious performance degradations in both BER and SNR are experienced when further increasing the launch power beyond 19 dBm, as shown in Fig. 5. This is attributed to the accumulated nonlinearity of the ~1.1-km FUT (i.e., SMF) in the 'SMF loop' after 20 loops. Specifically, the SNR performance degrades from ~13.5 dB to ~11.7 dB under a 23-dBm launch power after 20 loops.

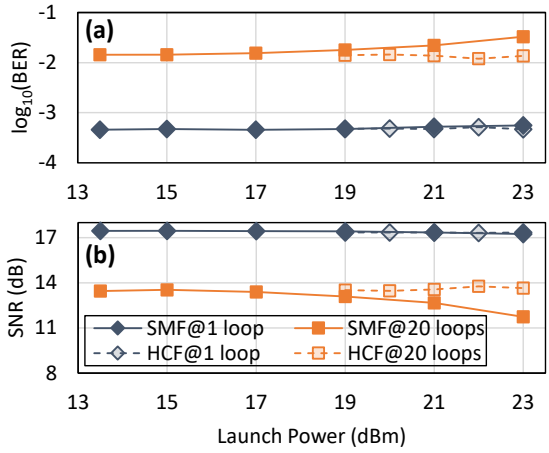

Fig. 5. Comparisons of 130-GBaud 16QAM transmission over the 'HCF loop' and 'SMF loop': (a) BER versus launch power, and (b) SNR versus launch power.

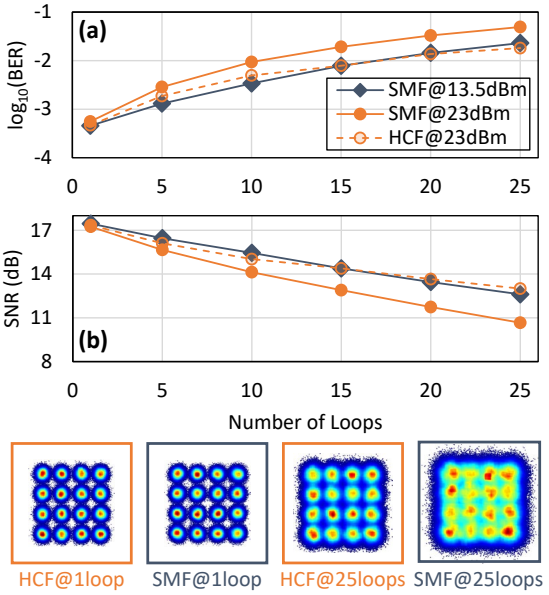

Fig. 6. Comparisons of 130-GBaud 16QAM transmission over the 'HCF loop' and 'SMF loop': (a) BER versus number of loops, and (b) SNR versus number of loops. Insets: constellation diagrams of the 'HCF loop' and 'SMF loop' after 1 loop and 25 loops when the launch power is 23 dBm.

We then kept the total launch power at the maximum 23 dBm (i.e., ~13.5 dBm/channel) and investigated the impact of fiber nonlinearity on both 'HCF loop' and 'SMF loop' after different numbers of loops. The corresponding BER and SNR results are given in Figs. 6(a) and 6(b), respectively, in which the performance of the 'SMF loop' with a 13.5-dBm launch power (at which the SMF's nonlinearity is considered as negligible) is included as a benchmark. As shown in Fig. 6, if the number of travelled loops is small, using a launch power of 23 dBm in the case of 'SMF loop' leads to a relatively minor performance

degradation when compared to that of the 13.5-dBm scenario. This is also evidenced by the similar constellation diagrams of the 'HCF loop' and 'SMF loop' after 1-loop transmission with a 23-dBm launch power, as presented as the insets in Fig. 6. However, the BER and SNR penalties tend to be significant when further increasing the number of loops, which results from the accumulated nonlinearity of the ~1.1-km FUT (i.e., SMF). In contrast, both the BER and SNR performances in the 23-dBm 'HCF loop' case are always comparable to that in the 13.5-dBm 'SMF loop' case, confirming that the HCF is capable of accommodating nonlinearity-free transmission despite the high launch power. Consequently, the SNR of the 130-GBaud 16QAM transmission can be significantly improved by more than 2 dB (from ~10.7 dB to ~13 dB). For reference, the constellation diagrams of the 'HCF loop' and 'SMF loop' under a 23-dBm launch power after 25 loops are also presented as insets in Fig. 6, from which a significantly worse performance in the 'SMF loop' case can be directly observed.

B. 130-GBaud PCS-64QAM Transmission

In this sub-section, we present another set of transmission results of 130-GBaud PCS-64QAM with an entropy of 5.7 bit/symbol. The NGMI and AIR are used to assess the transmission performance over both 'HCF loop' and 'SMF loop'. Fig. 7 shows the performance of the 'HCF loop' under different launch power levels. Thanks to the ultra-low nonlinearity of the HCF, as shown in Fig. 7(a), constant NGMI performance can be achieved regardless of the level of launch power in all three loop scenarios (i.e., transmission after 1 loop, 10 loops, and 25 loops). Accordingly, the same tendency is achieved by the AIR performance as shown in Fig. 7(b), validating again that the HCF can deliver nonlinearity-free transmission. Specifically, under a 23.5-dBm launch power, the NGMI values are around 0.94 and 0.74 after 1-loop and 25-loop transmission, which correspond to AIRs of ~1.39 Tb/s and ~1.08 Tb/s, respectively.

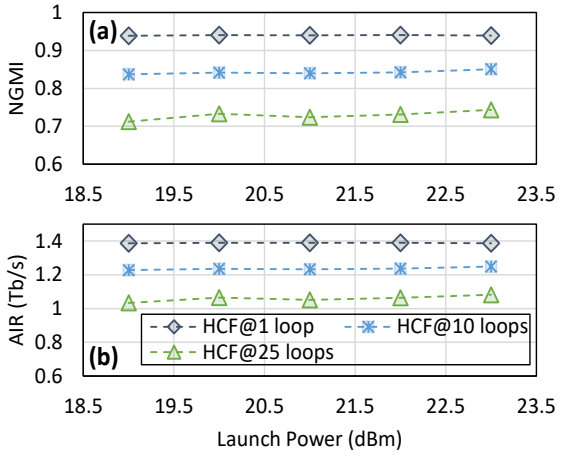

Fig. 7. Performance of 130-GBaud PCS-64QAM transmission over the optical recirculating loop: (a) NGMI versus launch power, and (b) AIR versus launch power.

The comparisons of the NGMI and AIR performances of between the 'HCF loop' and 'SMF loop' after 1 loop and 20 loops are presented in Fig. 8(a) and Fig. 8(b), respectively. For transmission after only 1 loop, similar NGMI and AIR performances can be achieved for launch powers up to 23 dBm in both the 'HCF loop' and 'SMF loop'. This again is because of the insignificant nonlinearity impact of the ~1.1-km FUT in both cases (i.e., either HCF or SMF). However, the FUT's nonlinearity gets accumulated as the number of loops increases, and if the nonlinearity is not sufficiently low, it will eventually impose non-negligible performance degradation on the transmission. This is directly reflected by the results of the 20-loop transmission in Fig. 8.

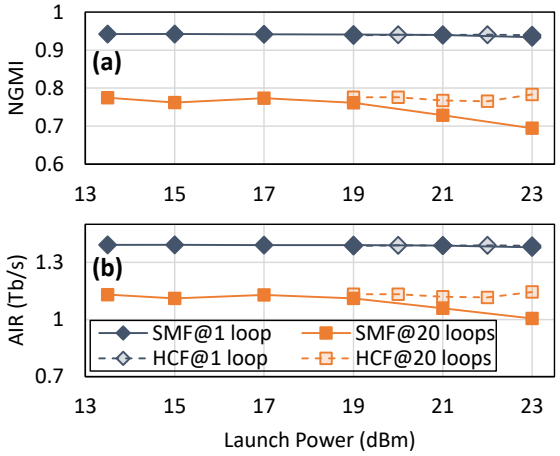

Fig. 8. Comparisons of 130-GBaud PCS-64QAM transmission over the 'HCF loop' and 'SMF loop': (a) NGMI versus launch power, and (b) AIR versus launch power.

It is seen that in the case of 'HCF loop', owing to the ultra-low nonlinearity of the HCF, the NGMI and AIR can always be maintained at around 0.77 and 1.13 Tb/s, respectively, despite the increase in launch power. In contrast, in the case of the 'SMF loop', comparable performance can only be achieved by using a launch power below 19 dBm. This is consistent with the results of the 16QAM transmission shown in Fig. 5. Further increasing the launch power results in a notable performance degradation due to the much higher nonlinearity of the ~1.1-km SMF (i.e., FUT in the 'SMF loop') relative to the HCF. Consequently, after 20 loops, a clear NGMI decrease is observed, which corresponds to an AIR reduction of ~0.14 Tb/s, as shown in Fig. 8.

Finally, the performance benefits of using the HCF relative to SMF under a 23-dBm launch power (~13.5 dBm/channel) are evaluated over different numbers of loops, and the results are illustrated in Fig. 9. As expected, the 23-dBm 'HCF loop' case exhibits comparable NGMI and AIR performances to that of the 13.5-dBm 'SMF loop' case, thanks to the low nonlinearity of the HCF. Furthermore, under a 23-dBm launch power, the 'SMF loop' suffers obvious performance degradations due to the SMF's nonlinearity. As shown in Fig. 9, the NGMI and AIR penalties become more significant as the number of travelling loops increases. By using the HCF instead of SMF as the FUT in the loop, after 25-loop transmission under a 23-dBm launch power, the NGMI can be improved to ~0.74. This corresponds to ~17.4% AIR improvement (from ~0.92 Tb/s to 1.08 Tb/s). For reference, the constellation

diagrams of the 'HCF loop' and 'SMF loop' after 1-loop and 15-loop transmission are presented as insets in Fig. 9 as well.

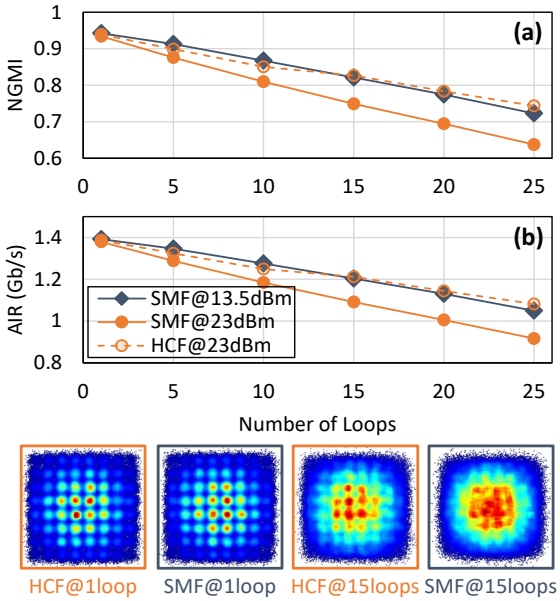

Fig. 9. Comparisons of 130-GBaud PCS-64QAM transmission over the 'HCF loop' and 'SMF loop': (a) NGMI versus number of loops, and (b) AIR versus number of loops. Insets: constellation diagrams of the 'HCF loop' and 'SMF loop' after 1 loop and 15 loops when the launch power is 23 dBm.

IV. Comparison of Latency Performance

In this section, we discuss another inherent benefit of the HCF – the ultra-low latency. This is evidenced by the power monitoring traces of the optical recirculating loop, as well as the results obtained through a field trial using a hollow-core cable.

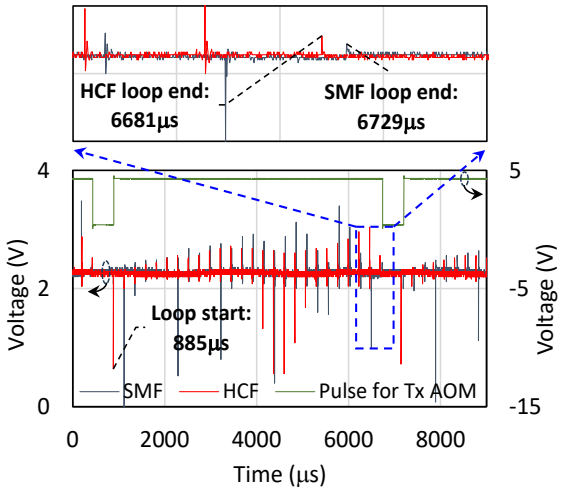

Fig. 10. Comparison of the power monitoring traces of the 'HCF loop' and 'SMF loop' after 25 loops.

Fig. 10 compares the power monitoring traces of the 25-loop 'HCF loop' and 'SMF loop', in which the maximum number of recirculation loops was controlled by the complementary pulses for the AOMs. The spikes induced by the transition of the AOM can be used to identify the end of each loop. We note that the loading stage of the recirculating loop was set to twice of the single-loop time. Therefore, the loop start/end can be identified by finding the end/start of the loading stage. As aforementioned, the only difference between the two loop cases is the type of fiber used for the ~1.1-km FUT (i.e., either HCF or SMF). Therefore, any latency difference between the two cases should be attributed to the contribution arising from the FUT. Therefore, in this way, the latency difference between HCF and SMF can be directly evaluated. From Fig. 10, the total propagation time of the 'HCF loop' and 'SMF loop' are calculated as 5,796 μs and 5,844 μs, respectively. These can be translated into fiber latencies of ~3.3 μs/km and ~5 μs/km for HCF and SMF, respectively, suggesting that HCF offers >30% latency reduction compared to the SMF.

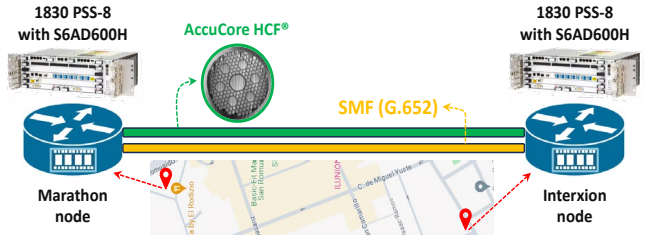

Fig. 11. Illustration of the HCF cable-based field trial.

TABLE I
Summary of the Field Trial using 90.22-GBaud 16QAM Signals

Cable Type	Pre-FEC BER	Round-trip Service Latency
G.652	1.51E-3	78.358 μs
AccuCore	1.55E-3	74.071 μs

We have also performed a field trial in Lyntia's backbone network between the Marathon node and the Interxion node in Madrid, Spain. As shown in Fig. 11, Nokia 1830 PSS-8 platforms with S6AD600H transponders were adopted to transmit and detect the 90.22-GBaud 16QAM signal at 1562.79 nm for the 600G trial, through which 100G real-time Ethernet services were enabled. A HCF (AccuCore HCF®) and a SMF (G.652, with a matched loss to the HCF using a VOA) were packed in the same OFS cable (around 1.38 km) and deployed in the field. With the same transmitted optical power (~0.57 dBm), the received optical powers were -10.52 dBm and -10.64 dBm for the HCF and SMF, respectively. Table I summarizes the BER and round-trip latency performances of the 100G services. Note that the service latency includes both the propagation time of the transmission fiber and the processing time of the transponders. While similar BERs are achieved by the HCF and SMF links, a round-trip latency reduction of 4.287 μs is realized by the HCF link. This validates that the HCF can offer a significant latency reduction of 1.553 μs/km. We note that since both the HCF and SMF are incorporated within the same cable, their physical length is known to be almost identical. Therefore, unlike the latency characterizations of the loop experiments which may be affected by the less accurate measurements of the in-loop fiber lengths, the latency reduction obtained in our field trial should be independent of length related errors. Nevertheless, the latency reduction results of our lab experiments and field trial agree well. Our field trial results

clearly highlight the practical viability of using the HCF for latency-sensitive and high-capacity connectivity.

V. Conclusions

In this paper, we present a comparative study based on an optical recirculating loop using either the HCF or SMF as the FUT inside the loop, through which we showcase the low nonlinearity and low latency of the HCF relative to SMF. It has been validated via both DP-16QAM and DP-PCS-64QAM transmission at 130 GBaud that the use of HCF allows for nonlinearity-free transmission under launch power levels up to 23 dBm (~13.5 dBm/channel). We demonstrate that by using the HCF instead of SMF, after 25-loop transmission under a 23-dBm launch power, significant performance improvements can be achieved, including >2-dB higher SNR and ~17.4% AIR enhancement. Furthermore, it is shown through the recirculating loop that the HCF can provide >30% latency reduction compared to SMF. A field trial of 90.22-GBaud 16QAM transmission over a ~1.4-km length of field-deployed HCF cable has also been conducted, verifying the practical feasibility of using the HCF for high-capacity transmission with ~1.6-μs/km latency reduction. Our results clearly indicate the promising potential of incorporating HCFs with the state-of-the-art high baud-rate coherent transceivers for future low-latency and ultrahigh-capacity optical communications.

References

[1] P.J. Winzer, D.T. Neilson, and A.R. Chraplyvy, "Fiber-optic Transmission and Networking: The Previous 20 and The Next 20 Years," *Opt. Express*, vol. 26, no. 18, pp. 24190-24239, 2018.

[2] E. Agrell, M. Karlsson, F. Poletti, *et al*., "Roadmap on Optical Communications," *J. Opt*., vol. 26, 093001, pp. 1-64, 2024.

[3] T. Fehenberger, A. Alvarado, G. Böcherer, *at al*., "On Probabilistic Shaping of Quadrature Amplitude Modulation for the Nonlinear Fiber Channel," *J. Lightw. Technol*., vol. 34, no. 21, pp. 5063-5073, 2016.

[4] B.J. Puttnam, G. Rademacher, and R.S. Luís, "Space-division Multiplexing for Optical Fiber Communications," *Optica*, vol. 8, no. 9, pp. 1186-1203, 2021.

[5] J. Renaudier, A. Napoli, M. Ionescu, *et al*., "Devices and Fibers for Ultrawideband Optical Communications," *Proc. IEEE*, vol. 110, no. 11, pp. 1742 -1759, 2022.

[6] Y. Hong, N. Taengnoi, K.R.H. Bottrill, *et al*., "Towards Ultra-wideband Optical Communications Using Novel Optical Amplifiers," in *Proc. of ACP*, Wuhan, China, paper ACPPOEM-0904-1, 2023.

[7] A.D. Ellis, J. Zhao, and D. Cotter, "Approaching the Non-linear Shannon Limit," *J. Lightw. Technol*., vol. 28, no. 4, pp. 423-433, 2010.

[8] A.C. Meseguer, J.T. de Araujo, and J.-C. Antona, "Multi-core vs Hollow-core Fibers: Technical Study of Their Viability in SDM Power-constrained Submarine Systems," *J. Lightw. Technol*., vol. 41, no. 12, pp. 4002-4009, 2023.

[9] Y. Sagae, T. Matsui, K. Tsujikawa, *et al*., "Solid-type Low-latency Optical Fiber with Large Effective Area," *J. Lightw. Technol*., vol. 37, no. 19, pp. 5028-5033, 2019.

[10] E.N. Fokoua, S.A. Mousavi, G.T. Jasion, *et al*., "Loss in Hollow-core Optical Fibers: Mechanisms, Scaling rules, and Limits," *Adv. Opt. Photon*., vol. 15, no. 1, pp. 1-85, 2023.

[11] B.J. Mangan, M. Kuschnerov, J.W. Nicholson, *et al*., "First Demonstration of Hollow-core Fiber for Intra Data Center Low Latency Connectivity with A Commercial 100Gb/s Interface," in *Proc. of OFC*, Los Angeles, USA, paper M3D.4, 2015.

[12] Y. Chen, M.N. Petrovich, E.N. Fokoua, *et al*., "Hollow Core DNANF Optical Fiber with <0.11 dB/km Loss," in *Proc. OFC*, San Diego, United States, paper Th4A.8, 2024.

[13] D. Ge, S. Gao, M. Zuo, *et al*., "Estimation of Kerr Nonlinearity in an Anti-resonant Hollow-core Fiber by High-order QAM Transmission," in *Proc. OFC*, San Diego, United States, paper W4D.6, 2023.

[14] A. Iqbal, P. Wright, N. Parkin, *et al*., "First Demonstration of 400ZR DWDM Transmission through Field Deployable Hollow-core-fibre Cable," in *Proc. of OFC*, San Francisco, United States, paper F4C.2, 2021.

[15] D. Ge, S. Gao, M. Zuo, *et al*., "Nonlinear-penalty-free Real-time 40×800Gb/s DP-64QAM-PCS Transmission with Launch Power of 28 dBm over a Conjoined-tube Hollow-core Fiber," in *Proc. of OFC*, San Diego, United States, paper W4H.7, 2023.

[16] C. Li, Z. Liu, Y. Sun, *et al*., "C-band Net 1.8 Tb/s (240Gb/s/λ× 8λ) DWDM IM/DD Transmission over 1.4km AR-HCF with Linear FFE Only," in *Proc. of OFC*, San Diego, United States, paper Tu3H.6, 2024.

[17] H. Chen, X. Zhang, Z. Liu, *et al*., "First Demonstration of Quasi-Continuous S+C+L 154.5 Tbit/s Coherent Transmission in Hollow-Core Anti-Resonant Fiber," in *Proc. of ACP*, Wuhan, China, paper ACPPOEM-1008-18, 2023.

[18] B. Zhu, B.J. Mangan, T. Kremp, *et al*., "First Demonstration of Hollow-core-fiber cable for Low Latency Data Transmission," in *Proc. of OFC*, San Diego, United States, paper Th4B.3, 2020.

[19] H. Yang, M. Xiang, X. Yu, *et al*., "Coherent WDM Transmission Over NANF for High-Capacity Intra-Data-Center Interconnection," *IEEE J. Sel. Top. Quantum Electron*., vol. 30, no. 6, 4300309, 2024.

[20] Y. Hong, T.D. Bradley, N. Taengnoi, *et al*., "Hollow-Core NANF for High-Speed Short-Reach Transmission in the S+C+L-Bands," *J. Lightw. Technol.*, vol. 39, no. 19, pp. 6167-6174, 2021.

[21] A. Saljoghei, M. Qiu, S.R. Sandoghchi, *et al*., "First Demonstration of Field-Deployable Low Latency Hollow-core Cable Capable of Supporting >1000km, 400Gb/s WDM Transmission," arXiv:2106.05343, 2021. [online]. Available: https://arxiv.org/abs/2106.05343.

[22] Y. Hong, K.R.H. Bottrill, T.D. Bradley, *et al.*, "Low-latency WDM Intensity-modulation and Direct-detection Transmission Over >100 km Distances in a Hollow Core Fiber," *Laser Photonics Rev.*, vol. 15, paper 2100102, 2021.

[23] M. Kuschnerov, V.A.J.M. Sleiffer, Y. Chen, *et al*., "Data Transmission through up to 74.8 km of Hollow-core Fiber with Coherent and Direct-detect Transceivers," in *Proc. of ECOC*, Valencia, Spain, paper Th. 1.2.4, 2015.

[24] A. Nespola, S.R. Sandoghchi, L. Hooper, *et al*., "Ultra-long-haul WDM Transmission in a Reduced Inter-modal Interference NANF Hollow-core Fiber," in *Proc. of OFC*, San Francisco, USA, paper F3B.5, 2021.

[25] A. Nespola, S.R. Sandoghchi, L. Hooper, *et al*., "Ultra-long-haul WDM PM-16QAM Transmission in a Reduced Inter-modal Interference NANF," in *Proc. of IPC*, Orlando, USA, paper WB1.3, 2023.

[26] Y. Hong, S. Almonacil, H. Mardoyan, *et al*., "Demonstration of Beyond Terabit/s/λ Nonlinearity-free Transmission over the Hollow-core Fibre," in *Proc. of ECOC*, Frankfurt, Germany, paper Th1B.4, 2024.

[27] OFS AccuCore HCF™ Optical Cable Solution. Accessed on Jan. 07, 2025, [online]. Available: https://www2.ofsoptics.com/accucore-hcf.

[28] J.M. Fini, J.W. Nicholson, R.S. Windeler, *et al*., "Low-loss hollow-core fibers with improved single-modedness," *Opt. Express*, vol. 21, no. 5, pp. 6233-6242, 2013.

[29] A. Ghazisaeidi, I.F.J. Ruiz, R. Rios-Müller, *et al*., "Advanced C+L-Band Transoceanic Transmission Systems Based on Probabilistically Shaped PDM-64QAM," *J. Lightw. Technol.*, vol. 35, no. 7, pp. 1291-1299, 2017.